

SPECTRAL VARIATIONS IN EARLY-TYPE GALAXIES AS A FUNCTION OF MASS

KRISTI DENDY CONCANNON AND JAMES A. ROSE

Department of Physics and Astronomy, CB #3255, University of North Carolina, Chapel Hill, NC 27599

AND

NELSON CALDWELL

F. L. Whipple Observatory, Smithsonian Institution, P.O. Box 97, Amado, AZ 85645

Draft version October 29, 2018

ABSTRACT

We report on the strengths of three spectral indicators — Mg₂, H β , and Hn/Fe — in the integrated light of a sample of 100 field and cluster E/S0 galaxies. The measured indices are sensitive to age and/or metallicity variations within the galaxy sample. Using linear regression analysis for data with non-uniform errors, we determine the intrinsic scatter present among the spectral indices of our galaxy sample as a function of internal velocity dispersion. Our analysis indicates that there is significantly more intrinsic scatter in the two Balmer line indices than in the Mg₂ index, indicating that the Balmer indices provide more dynamic range in determining the age of a stellar population than does the Mg₂ index. Furthermore, the scatter is much larger for the low velocity dispersion galaxies, indicating that star formation has occurred more recently in the lower mass galaxies.

Subject headings: galaxies:abundances— galaxies:stellar content

1. INTRODUCTION

An enormous effort has been made in recent years to disentangle the degenerate effects of age and metallicity on the integrated light of a galaxy. This age-metallicity degeneracy (Worthey 1994, 1996) plagues both the photometric colors and the integrated spectrum of a galaxy, making it extremely difficult to separate the effects of the two. Because broadband colors cannot break the degeneracy (Bica et al. 1990; Charlot & Silk 1994), the best way to determine a unique solution to the problem is to use a combination of population synthesis models and spectral line indices. Absolute ages and metallicities determined using this method are naturally subject to systematic errors, yet relative values are still of great interest and are generally more reliable (e.g., Trager et al. 2000a). Although no single spectral index can completely separate the effects of age and metallicity, it is possible to determine the relative range empirically by plotting a single spectral index with a predominant age or metallicity sensitivity versus a mass indicative parameter such as the absolute magnitude or internal stellar velocity dispersion. The spread in index values which is observed as a function of mass is then directly related to the range in age and/or metallicity in the galaxy sample.

The most widely used spectral index system is the set of indices originally defined in Burstein et al. (1984) and further refined in Worthey et al. (1994) and Trager et al. (1998), now commonly known as the Lick system. In this system, the H β index is used as the primary age-sensitive spectral indicator, whereas the Mg and Fe indices are used as the primary metallicity indicators. Using the Lick indices, many groups have been able to place constraints on the ages and metallicities of various galaxy samples. For example, Trager et al. (2000a) find that for a sample of early-type galaxies in low density environments there

is a large spread in H β values (i.e., age), but very little variation in metallicity. For galaxies in the Fornax cluster, though, Kuntschner (2000) finds the opposite effect, in that a large spread in metallicity is present with little variation in age. Whether such contrasting results are a product of the different environments in the two samples is an interesting and still unanswered question. It is clear, however, that a comparison of the range in age and metallicity of galaxies in different environments will lead to a better understanding of the parameters which govern the evolution of galaxies.

To constrain galaxy evolution scenarios, it is imperative that we first derive reliable values for the ages and metallicities of galaxies. In this paper we present first results of a sample of 100 early-type galaxies covering a large baseline in mass and a large range in wavelength in order to use both the Lick/IDS age/metallicity indicators as well as additional indices centered around the higher order Balmer lines. Although the data will eventually be used to determine absolute ages and metallicities, and thereby place constraints on the theories governing galaxy formation and evolution, these goals are beyond the scope of this paper. In this letter, we demonstrate the importance of the lower mass galaxies and higher order Balmer lines for obtaining a complete view of the ages of early-type galaxies. The paper is organized such that the data and reduction procedures are summarized in §2, the spectral indices and the index diagrams are presented in §3, and the analysis of these diagrams is given in §4 and discussed in §5.

2. OBSERVATIONS

Our galaxy sample consists of 100 early-type galaxies, 70 of which are field galaxies and 30 of which are in the Virgo cluster. The field galaxies are drawn from the CfA redshift survey (Huchra et al. 1983); the cluster galaxies are from the Virgo Cluster Catalog (VCC) of Binggeli et

al. (1985). The observed galaxies cover a range in absolute magnitude of $-16 < M_B < -22$ and have been previously classified as either E or S0.

Long slit spectra of the galaxies were obtained at the F. L. Whipple Observatory with the 60" Tillinghast telescope, the FAST spectrograph and a Loral 512 x 2688 pixel CCD (Fabricant et al. 1998) during seven different observing runs between 1997 September and 1999 October in seeing conditions of 1" or better. A 3" slit and the 600 line/mm grating were used to give a dispersion of 0.75Å/pixel and 3Å FWHM spectral resolution and a spectral coverage of 3500Å - 5500Å. Each exposure was 1800 seconds with 2-4 exposures taken for each galaxy. The slit was oriented at the parallactic angle so as to preserve the blue light, resulting in a S/N per pixel between 70 and 100 at 4000Å in the final coadded spectrum.

The spectra were reduced in IRAF with standard reduction procedures including bias and dark subtraction as well as flat fielding. The spectra were wavelength calibrated using an internal HeNeAr lamp and were flux calibrated using standard stars from the Massey et al. (1988) spectrophotometric catalog. Multiple galaxy exposures were added together and all galaxies were de-redshifted to the same rest wavelength. Velocity dispersions were determined using the Fourier cross-correlation method (e.g., Tonry & Davis 1979) in the task *fxcor* and various stellar templates which were observed during twilight. All spectra were then smoothed to the same effective dispersion of 230 km/s to insure that each object experienced the same intrinsic broadening.

3. SPECTRAL INDICES

Two types of spectral indices were measured from the calibrated and smoothed spectra, the pseudo-equivalent width indices of the Lick group (Burstein et al. 1984; Worthey et al. 1994) and the line ratios of Rose (1994; Caldwell & Rose 1998). The Lick/IDS family of indices measures the pseudo-equivalent width of absorption line features such as H β and the Mg bands which lie redward of 4000Å. The Lick equivalent width indices are measured by centering a bandpass of typically 30-40Å on the absorption feature and using a red and blue sideband of similar width as the continuum reference. In addition to the Lick system, we have also chosen to work at bluer wavelengths where young stars contribute a larger fraction of the light. The indices used in this region are the Rose spectral line ratios, which are defined as the ratio of the residual intensity in two neighboring spectral lines. For our galaxy sample, we have measured a total of 36 spectral indices, 22 Lick indices and 14 Rose indices, and report in this letter on three of the key age/metallicity diagnostics. The spectral indices analyzed here are: Mg₂, a Lick index which measures the strength of the Mg H + Mg b molecular bands, H β , another Lick index which measures the equivalent width of the H β feature at 4861Å, and Hn/Fe, a Rose spectral line index which is an average of three hydrogen to iron line ratios¹ and is defined such that a lower index value corresponds to a stronger Balmer line strength.

For each index, the error for an individual galaxy is determined from the rms scatter in the repeat measurements. Since this method is unreliable for those galaxies

which have only two observations, we have defined our errors for a particular index and galaxy utilizing the errors in all indices and galaxies in the following manner. The error, Λ_{ij} , in index j for galaxy i (where there are a total of m indices and n galaxies) is given by:

$$\Lambda_{ij} = \frac{\sum_{i=1}^n \varepsilon_{ij} \sum_{j=1}^m \varepsilon_{ij}}{\sum_{i,j=1}^{m,n} \varepsilon_{ij}} \quad (1)$$

where $\sum_{i=1}^n \varepsilon_{ij}$ is the rms error in the j^{th} index averaged over all galaxies, $\sum_{j=1}^m \varepsilon_{ij}$ is the error in the i^{th} galaxy averaged over all indices of the same type (i.e., all Lick indices or all Rose indices), and $\sum_{i,j=1}^{m,n} \varepsilon_{ij}$ is the average error in all indices of the same type for all galaxies. The average fractional uncertainty in each index is 1% for Hn/Fe and Mg₂, 3% for H β and 2% for the velocity dispersion measurements.

The three indices reported in this paper are shown in Figure 1 as a function of $\log \sigma$ (i.e., as a function of mass). The line is the best fit to the high-mass data extended to the low-mass end; an explanation of this fit is given in §4. Comparing these diagrams, two effects are immediately evident. First, the scatter among galaxies appears to increase between the high-mass end and the low-mass end of the diagrams. Second, this increase in scatter is significantly more dramatic in both the H β and Hn/Fe diagrams than it is in the Mg₂ diagram. Some of the observed scatter of the galaxies about the linear fits is obviously due to measurement errors associated with the data, but variations in the age and metallicity of the galaxies play a contributing role as well, and in practice, it is difficult to separate this intrinsic scatter from the observational errors. In the following section, we describe a statistical analysis of the scatter in the index diagrams and discuss their implications.

4. RESULTS

In each diagram in Figure 1, a linear relation is readily identifiable for the galaxies with $\log \sigma > 2.0$. This property is related to the well-known color-magnitude relation of elliptical galaxies (Visvanathan & Sandage 1977) and is thought to be driven by metallicity (Faber 1973, 1977). The relation is naturally explained by the supernova-driven wind model (Larson 1974; Arimoto & Yoshii 1987) in which the more massive galaxies are better able to retain their supernova ejecta than the smaller galaxies and thus become more metal-rich and redder. Because the high-mass galaxies represent a fiducial, normal sample of galaxies, we used only these points to determine the best fit to the data and extended the fit to the lower mass galaxies. The three outlying points above $\log \sigma = 2.0$ were not used in the regression analysis, since each of these galaxies is known to be in an interacting system with star formation, possibly triggered by this interaction. The least-squares fitting is done using the BCES (bivariate correlated errors and intrinsic scatter) method of Akritas & Bershady (1996) that fits data for which there is some intrinsic scatter present and for which the error bars are heteroscedastic (non-uniform) in both the x and y coordinates. Because we are interested in measuring the intrinsic scatter as a function of mass (i.e., internal velocity dispersion), the chosen fit minimizes the residuals in the indices

¹ $Hn/Fe = < H\delta/Fe4045 + H\gamma/Fe4325 + H8/Fe3859 >$

(y -variables), which have, on average, larger errors than the velocity dispersion (x -variable). To verify the fits, the analysis was repeated for 1000 bootstrap re-samplings of the data. We find that the BCES and bootstrap fits agree within their associated errors.

To separate the intrinsic scatter, η , from the scatter due to measurement errors, we used an estimate given by Fioc & Rocca-Volmerange (1999):

$$\eta^2 = \sum [(y_i - Bx_i - A)^2 - (B^2 \xi_{xi}^2 + \xi_{yi}^2)] \quad (2)$$

where B and A are the slope and intercept respectively of the BCES regression analysis, x_i is the observed $\log \sigma$, y_i is the observed index value and ξ_{xi} , ξ_{yi} are the associated errors in the x_i and y_i observations. The galaxies were divided into two bins, $\log \sigma > 2.0$ and $\log \sigma < 2.0$, the scatter was calculated for each subsample, and the analysis was verified with Monte-Carlo simulations. The measured intrinsic scatter for both the high- and low-mass subsamples is shown as the vertical dotted lines in the lower right corners of Figure 1.

The results of the statistical analysis of the three spectral indices, $H\beta$, Mg_2 , and Hn/Fe , are shown in Table 1. Here, the intrinsic scatter in each subsample is denoted by η ; the error in η , estimated from bootstrap re-samplings, is given by δ_η . The reader should be aware that because the two Lick indices and the Rose index are defined differently (as equivalent widths and a line ratio, respectively) it is not meaningful to compare the absolute difference in the intrinsic scatter between two indices, i.e., it is only meaningful to compare relative differences in the same index. The quantitative analysis clearly verifies our previous predictions in that a non-zero intrinsic scatter exists in each of the index diagrams and that this scatter is greater for the low-mass galaxies than for the high-mass galaxies. In fact, the intrinsic scatter increases by a factor of 1.5 from the low-mass to the high mass galaxies in the Mg_2 diagram, by a factor of 2.6 in the $H\beta$ diagram, and by a factor of 5.2 in the Hn/Fe diagram (R value in Table 1). In addition to the three indices reported here, we have also estimated the intrinsic scatter in another Lick index, Mg b, which has become a popular age/metallicity indicator (e.g., Trager et al. 2000a). For this index, we find that the intrinsic scatter increases by a factor of 2.2 from the high-mass to the low-mass galaxies. It is worth noting that this value is between the estimates for Mg_2 and $H\beta$.

From this analysis, it is evident that more intrinsic scatter exists in the Balmer indices than in the Mg_2 index. If the factor driving the scatter were metallicity instead of age, we would actually expect to see a larger scatter in the Mg_2 data than in the Balmer indices, since Mg_2 is more sensitive to metallicity than to age in comparison with $H\beta$ and other Balmer lines (e.g., Buzzoni et al. 1994). However, the opposite situation is observed. Because we see more variations in the Balmer indices than the Mg_2 index, especially at low mass, the index diagrams imply that the

lower-mass galaxies exhibit a larger range in ages than the high-mass galaxies.

5. DISCUSSION

The results of this analysis bring forth two key issues that must be addressed. First, since the two Balmer line indices exhibit more intrinsic scatter than the Mg_2 index, this qualifies them as more robust age indicators. The relatively little intrinsic scatter observed in the Mg_2 -log σ diagram indicates that this index is not well suited for constraining the age of a stellar population. The fact that significant age variations may be hidden in the Mg_2 -log σ relation has been previously noted by both Worthey et al. (1996) and Jørgensen (1999) and has been studied in detail by Trager et al. (2000b). This finding may have a significant impact on the previous results of authors who have used the Mg_2 index as their principal age diagnostic (e.g., Bernardi et al. 1998), and their conclusions may need to be re-evaluated using a more age-sensitive index such as $H\beta$ or Hn/Fe .

The second key result is the amount of scatter observed for the low-mass galaxies in the index diagrams. The dramatic increase in scatter, particularly at the low-mass end of the Balmer line diagrams, indicates that the smaller galaxies have experienced a more varied star formation history and that these galaxies have a larger range in age than their brighter counterparts. This finding places significant constraints on a hierarchical formation scenario such as the CDM model (Baugh, Cole & Frenk 1996; Kauffmann 1996), since in this case one would naively expect to see that low-mass galaxies are older than the larger galaxies (Kauffmann & Charlot 1998). However, because the majority of the low-mass galaxies in our sample are in the Virgo cluster, it is difficult to determine whether the observed variation in age is simply a product of the different environments. Even if this were the case, though, in a hierarchical scenario we would expect that galaxies in clusters would be older than field galaxies, since merging will happen more rapidly in clusters. Thus, regardless of the environmental influence, our results appear to place significant constraints on the hierarchical picture.

In a forthcoming paper, we will report on use of the higher order Balmer index and population synthesis models to determine the spread of age and metallicity of our sample, and thereby place quantitative constraints on formation and evolution scenarios.

We would like to thank to William J. Thompson for much valuable advice and discussion concerning the statistical analysis in this paper. Thanks are also due to Michael Akritas and the SCCA² for their advice. This research was supported in part by a North Carolina NASA Space Grant Consortium Graduate Fellowship and by NSF grant AST-9900720 to the University of North Carolina.

REFERENCES

Akritas, M. G., & Bershady, M. A. 1996, ApJ, 470, 706
 Arimoto, N., & Yoshii, Y. 1987, A&A, 173, 23
 Baugh, C. M., Cole, S., & Frenk, C. S. 1996, MNRAS, 283, 1361

Bernardi, M., Renzini, A., Da Costa, L. N., Wegner, G., Alonso, M. V., Pellegrini, P. S., Rite, C., & Willmer, C. N. A. 1998, ApJ, 508, L43
 Binggeli, B., Sandage, A., & Tammann, G. A. 1985, AJ, 90 1681

²<http://www.stat.psu.edu/~mga/scca/>

Bica, E., Alloin, D., & Schmidt, A. 1990, A&A, 228, 23

Burstein, D., Faber, S. M., Gaskell, C. M., & Krumm, N. 1984, ApJ, 287, 586

Buzzoni, A., Mantegazza, L., & Gariboldi, G., 1994, AJ, 107, 513

Caldwell, N., & Rose, J. A., 1998, AJ, 115, 1423

Charlot, S., & Silk, J. 1994, ApJ, 432, 453

Faber, S. M. 1973, ApJ, 179, 731

Faber, S. M. 1977, in The Evolution of Galaxies and Stellar Populations: conference at Yale University, May 19-21, 1977, ed. B. M. Tinsley and R. B. Larson (New Haven, Conn.:Yale Observatory)

Fabricant, D., Cheimets, P., Caldwell, N., & Geary, J. 1998, PASP, 110, 79

Fioc, M., & Rocca-Volmerange, B. 1999, A&A, 351, 869

Huchra, J., Davis, M., Latham, D., & Tonry, J. 1983, ApJS, 52, 89

Jørgensen, I. 1999, MNRAS, 306, 607

Kauffmann, G. 1996, MNRAS, 281, 487

Kauffmann, G., & Charlot, S. 1998, MNRAS, 297, 23

Kuntschner, H. preprint (astro-ph/0001210)

Larson, R. B. 1974, MNRAS, 169, 229

Massey, P., Strobel, K., Barnes, J. V., & Anderson, E. 1988, ApJ, 328, 315

Rose, J. A., 1994, AJ, 107, 206

Tonry, J. & Davis, M., 1979, AJ, 84, 1511

Trager, S. C., Worthey, G., Faber, S. M., Burstein, D., & González, J. J. 1998, ApJS, 116, 1

Trager, S. C., Faber, S. M., Worthey, G., & González, J. J. 2000a, AJ, 119, 1645

Trager, S. C., Faber, S. M., Worthey, G., & González, J. J. 2000b, preprint (astro-ph/0004095)

Visvanathan, N., & Sandage, A. 1977, ApJ, 216, 214

Worthey, G. 1994, ApJS, 95, 107

Worthey, G. 1996, in IAU Symp. 171, New Light on Galaxy Evolution, ed. R. Bender and R. L. Davies (Dordrecht:Kluwer), 71

Worthey, G., Faber, S. M., Gonzalez, J. J., & Burstein, D. 1994, ApJS, 94, 687

Worthey, G., Trager, S. C., & Faber, S. M. 1996, in Fresh Views on Elliptical Galaxies, ed. A. Buzzoni, A. Renzini, & A. Serrano, A.S.P.Conf.Ser., vol. 86 (San Francisco: ASP), p.203

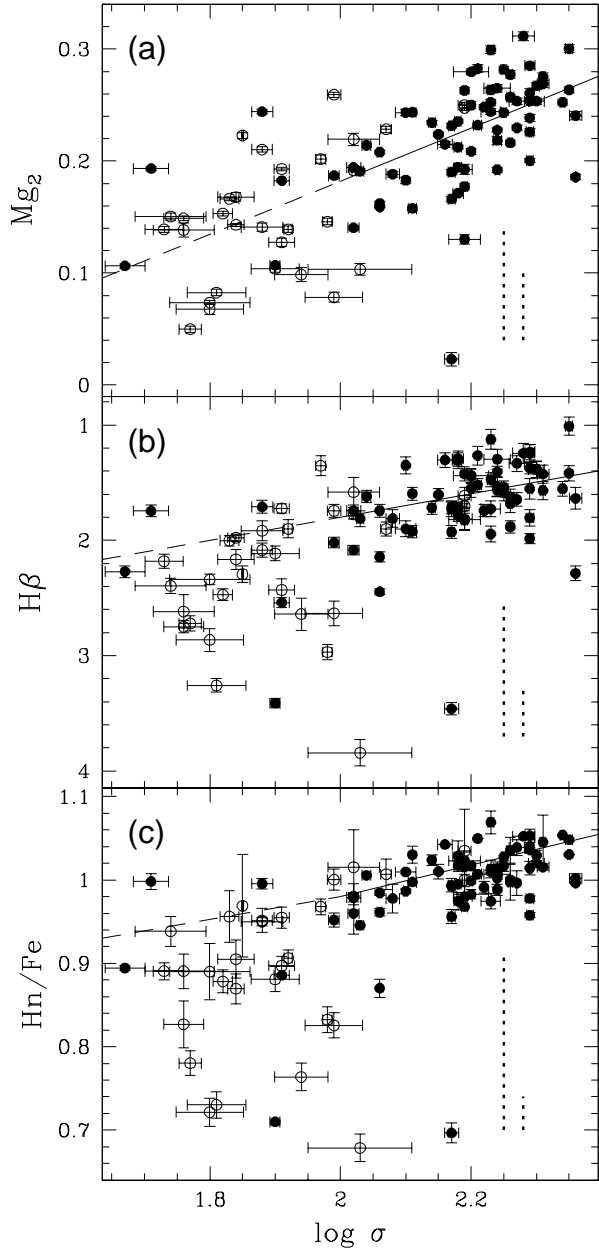


FIG. 1.— Three spectral indices (a) Mg_2 , (b) $H\beta$, (c) Hn/Fe plotted versus $\log \sigma$. The solid circles are field galaxies; the open circles are Virgo cluster galaxies. The regression line is the calculated fit with the dashed portion indicating the region of the line which is extrapolated. The vertical dotted lines represent the measured amount of intrinsic scatter in each subsample; the high-mass scatter is on the right, the low-mass scatter is on the left. The index values in (a) are in magnitudes; the values in (b) are equivalent widths in Angstroms; the index in (c) is a ratio.

TABLE 1
MEASURED INTRINSIC SCATTER IN INDEX DIAGRAMS

Index	Subsample ^a	η	δ_η	R ^b	δ_R ^c
Mg ₂	low mass	0.050	0.005	1.52	0.21
	high mass	0.033	0.003		
H β	low mass	0.578	0.084	2.60	0.48
	high mass	0.222	0.025		
Hn/Fe	low mass	0.105	0.015	5.25	1.01
	high mass	0.020	0.003		

^aLow mass: $\log \sigma < 2.0$; high mass: $\log \sigma > 2.0$

^bRatio of intrinsic scatter in low mass galaxies to that in high mass galaxies

^cError in the intrinsic scatter ratio